Rev. Acad. Colomb. Cienc. Ex. Fis. Nat. 44(173):974-983, octubre-diciembre de 2020
doi: https://doi.org/10.18257/raccefyn.1265

Original article

Mie scattering study of dielectric nanoparticles and nanoantennas applications

Estudio de la dispersión de Mie de nanopartículas dieléctricas y de las aplicaciones en nanoantenas

Oslen Dilayder Jaimes-Suárez*, Heriberto Peña-Pedraza

Universidad de Pamplona, Pamplona, Colombia

Abstract

The development of devices for focusing radiation on desired targets is of great importance in different fields of science and communication technologies as it would allow the creation of more efficient optical instruments. In this study, we explored the dispersion of dielectric spherical nanoparticles using elements from Mie's theory. There was evidence that the form of dispersed radiation patterns depends on factors such as the size of particles and the wavelength of incident radiation. The knowledge regarding radiation dispersion could be applied in the development of nanoantennas, as well as new nanotechnology devices and arrangements.

Keywords: Dielectric nanoparticles; Nanoantennas; Radiation pattern.

Resumen

El diseño de dispositivos capaces de enfocar la radiación de la manera deseada es de gran importancia en diferentes campos de la ciencia y la tecnología de la comunicación, y permitiría la creación de instrumentos ópticos más eficientes. En este estudio se exploró la dispersión de nanopartículas esféricas dieléctricas a partir de elementos de la teoría de Mie. Se pudo observar que la forma del patrón de radiación dispersa depende de factores como el tamaño de la partícula y la longitud de onda de la radiación incidente. El conocimiento sobre la dispersión de la radiación podría utilizarse en aplicaciones de nanoantenas, en el desarrollo de nuevos dispositivos y en arreglos de nanotecnología.

Palabras clave: Nanopartículas dieléctricas; Nanoantenas; Patrón de radiación.

Introduction

The development of optical circuits and nanoantennas promises to be a point of great importance for the proper functioning of ultrafast optical communication systems, in photonics science and the technology to generate, control, and detect light at a quantum level. This is possible by researching, designing, developing, and creating the elemental components of the various nanophotonic devices and their properties including scattering patterns through which the incident radiation can be precisely redirected or focused.

The variations of the refractive indexes of the dielectric material used in the manufacture of nanoparticles are among the components useful for controlling radiation direction. This can be done by varying the frequency of the incident wave or selecting an adequate particle size. In this context, **Tribelsky, *et al.*** (2015) studied the effects of the relation between the dipole and multipolar modes that produce anomalous scattering effects.

Many functional devices such as nano lenses, wave nano-guides, and nanoparticle-based nanoantennas can operate as optical devices. The main drawbacks of using metallic nanoparticles are their intrinsic losses, which strongly affect their general performance when used as optical devices. In terms of directionality, in metallic nanoparticles, the resonant scattering is dominated by resonances of the electric dipole type due to their

Citación: Jaimes-Suárez OD, Peña-Pedraza H. Mie scattering study of dielectric nanoparticles and nanoantennas applications. Rev. Acad. Colomb. Cienc. Ex. Fis. Nat. 44(173):974-983, octubre-diciembre de 2020. doi: https://doi.org/10.18257/raccefyn.1265

Editor: Pedro Fernández de Córdoba

***Correspondencia:**
Oslen Dilayder Jaimes Suarez;
oslen.jaimes@unipamplona.edu.co

Recibido: 9 de julio de 2020
Aceptado: 8 de septiembre de 2020
Publicado: 5 diciembre de 2020

plasmonic behavior. On the other hand, in the dielectric nanoparticles, the electric and magnetic dipole resonances predominate enabling an improvement in the directionality of the scattering (**Fu, *et al.,*** 2013).

Silicon dielectric nanoparticles exhibit sharp scattering due to the pronounced resonances associated with the excitations of the magnetic and electrical modes. Factors such as the high permittivity of the dielectric nanoparticle allow observing magnetic dipole resonance in the visible spectral range for silicon nanoparticles with radii of approximately 100 nm (**Evlyukhin, *et al.,*** 2012).

The study and development of optically resonant nanostructures for the control of far-field scattering through intermodal interference have been determined by the rapid progress in the field of nanophotonics. These effects are associated with plasmonic nanostructures. Based on this, a new branch of nanophotonics has emerged, which seeks to manipulate the strong Mie electronic and magnetic resonances optically produced in high refractive index dielectric nanoparticles. One of the reasons for the use of dielectric nanoparticles is that they reduce dissipative losses and, therefore, achieve a resonant improvement in electric and magnetic fields (**Kuznetsov, *et al.,*** 2016).

In the design and construction of resonant dielectric nanophotonic devices, silicon is generally maintained as a constituent material always due to its availability, low cost, and advanced technological treatment. The optical properties of silicon are almost ideal for a strong Mie resonant response, as it has a refractive index of 3.5 and negligible absorption losses in the telecommunications spectral range, thus presenting a significant magnetic dipole response. In addition to their exceptional optical properties, silicon nanostructures are mechanically and thermally exceptional (**Decker & Staude***,* 2016).

Nanoantennas behave in the same way as radio wave antennas, which are characterized by their ability to establish an efficient link between the near optical fields and the far-field of propagation. Thus, the nanoantennas can energetically improve the interaction of light with matter at the nanoscale due to their ability to efficiently link spatially located and propagated optical fields and, also, by giving fine characteristic directivity to the radiation and focusing and concentrating the electromagnetic fields at specific points with an enormous potential for applications ranging from light microscopy and nanoscale spectroscopy to the conversion of solar energy, integrated optical nanocircuits, and optoelectronics (**Biagioni, *et al.,*** 2012).

Maintaining control of light at the nanoscale has been a topic of particular interest due to the many emerging applications, such as 3D optical interconnections on multilayer chips, the improvement of fluorescence signals in bioimaging, high-resolution spatial light modulators, and concentration of light energy in heat-assisted magnetic recording. At the nanoscale, conventional optical elements are neither applicable nor useful for the development of nanodevices, therefore, current optical devices as nanoantennas offer a new conceptual approach with new geometries for non-classical light emission, harmonic generation, nanoscale photodetectors, and the detection of individual molecules (**Novotny *&* Van Hulst,** 2011).

The plasmonic nanoantennas studied in optics are still far from achieving the same characteristics that conventional antennas present at radio frequencies due to losses in metallic elements. For this reason, the use of fully dielectric nanoantennas is considered an alternative to plasmonic or metallic nanostructures. The use of dielectrics also has advantages such as low radiation loss, relatively small sizes, lightweight, high radiation efficiency, and reasonable bandwidth (**Mongia *&* Bhartia,** 1994).

The directivity in dielectric nanoparticles in some spectral wavelengths is possible because the particles can act as Huygens sources by scattering all radiation in the forward direction while other wavelengths of the electromagnetic radiation will be almost totally scattered backward (**Kerker, *et al.,*** 1983). This behavior is associated with Fano directional resonance, a type of resonance effect that helps to explain the existing asymmetry of directionality. The microscopic origin of this resonance arises from constructive and

Rev. Acad. Colomb. Cienc. Ex. Fis. Nat. 44(173):974-983, octubre-diciembre de 2020
doi: https://doi.org/10.18257/raccefyn.1265

destructive interference. Generally, this resonance is associated with quantum systems, but these wave function interference phenomena are also present in classical optics (**Luk'yanchuk, *et al.,*** 2003).

Materials and methods

We report here on the geometry of the radiation scattered by spherical silicon particles at nanometric scales using the Mie theory (**Luk'yanchuk, *et al.,*** 2003). When considering a nanoparticle as a nanoantenna, the particularities of each nanoparticle determine its intrinsic radiation patterns. In this way, it is possible to study the characteristics of gain and directivity of the radiation absorbed and scattered by spherical silicon nanoparticles.

For the visualization of the scattering patterns, we wrote a code in Python using the Mie theory to then calculate forward and backward scattering patterns. The Mie theory studies the characteristics of the scattering of electromagnetic radiation with the matter at the nanometer scale. To conduct the study, we reviewed the problem of a plane electromagnetic wave that impinges on a spherical particle where the wave induces an excitation in the electrons producing electronic oscillations and the energy of the incident electromagnetic wave can be scattered and absorbed by the particle. In dielectric nanoparticles, irradiated scattering occurs as a consequence of electrical and magnetic resonances resulting in a great variety of forms observable in the scattered radiation. The absorption (σ_{abs}), extinction (σ_{ext}), and scattering (σ_{dis}) cross-sections are written as (**Bohren & Huffman,** 2008):

$$\sigma_{dis} = \frac{2\pi}{k^2}\sum_{j=1}^{\infty}(2j+1)Re(a_j + b_j) \quad (1)$$

$$\sigma_{ext} = \frac{2\pi}{k^2}\sum_{j=1}^{\infty}(2j+1)\left(|a_j|^2 + |b_j|^2\right) \quad (2)$$

$$\sigma_{abs} = \sigma_{ext} - \sigma_{dis} \quad (3)$$

$$a_j = \frac{m\psi_j(mx)\psi_j'(x) - \psi_j(x)\psi_j'(mx)}{m\psi_j(mx)\xi_j'(x) - \xi_j(x)\psi_j'(mx)} \quad (4)$$

$$b_j = \frac{\psi_j(mx)\psi_j'(x) - m\psi_j(x)\psi_j'(mx)}{\psi_j(mx)\xi_j'(x) - m\xi_j(x)\psi_j'(mx)} \quad (5),$$

where k is the wave vector (m^{-1}); a_j, b_j are the scattering coefficients; x is the size parameter m, the ratio between the refractive indices of the nanoparticle and the medium, and $\psi_j(x)$, $\xi_j(x)$ are the Ricatti-Bessel functions defined as:

$$\psi_j(x) = \sqrt{\frac{\pi x}{2}}J_{j+\frac{1}{2}}(x) \quad (6)$$

$$\xi_j(x) = \sqrt{\frac{\pi x}{2}}\left[J_{j+\frac{1}{2}}(x) + iY_{j+\frac{1}{2}}(x)\right] \quad (7),$$

where $J_{j+\frac{1}{2}}(x)$ is the Bessel function of the first kind and $J_{j+\frac{1}{2}}(x)$ is the Bessel function of the second kind.

Using the angular components of the electric field scattered by the particle, it is possible to study the behavior and shape of the scattered radiation using the following equations:

$$S_1 = \sum_j \frac{2j+1}{j(j+1)}(a_j\pi_j + b_j\tau_j) \quad (8)$$

$$S_2 = \sum_j \frac{2j+1}{j(j+1)}(a_j\tau_j + b_j\pi_j) \quad (9)$$

$$\pi_j = \frac{P_j^1(cos\theta)}{sin\theta} \quad (10)$$

$$\tau_j = \frac{dP_j^1(cos\theta)}{d\theta} \quad (11),$$

where P_j^1 ($cos\theta$) corresponds to the associated Legendre polynomials of order 1 and degree j; $\boldsymbol{i}_{\parallel}$ is defined as the parallel scattered irradiance per unit of incident radiation, and $\boldsymbol{i}_{\perp}$ as the perpendicular scattered irradiance per unit of incident radiation:

$$i_{||} = |s_1|^2 \quad (12)$$

$$i_{\perp} = |s_2|^2 \quad (13)$$

For the angular dependence, the sums of the irradiances are plotted in polar and spherical coordinates varying Mie parameter given by:

$$x = \frac{2\pi r}{\lambda} \quad (14),$$

where λ is the wavelength of the incident radiation.

Results and discussion

In this work, we considered the use of free access computational tools with several codes implemented in Python for numerical calculation and the subsequent display of the results of the radiation patterns shown below.

Figure 1 shows the scattering cross-section of a spherical silicon particle with a radius of 80 nm in free space interacting with a plane electromagnetic wave; these spectra were calculated based on Mie's theory. The forward scattering spectra corresponds to the curve in blue color while backscattering spectra corresponds to orange color.

As shown in **figure 1**, both spectra have two well-defined peaks in the visible spectral range. The maximum of forward scattering spectra located around 520 nm is due to electrical resonances and the one close to 640 nm is due to magnetic resonances (**Kuznetsov, *et al.*,** 2012).

Furthermore, the maximum values of the electrical and magnetic resonances of the backscattering spectrum are located closer to each other compared to the forward. For wavelengths higher than 635 nm and values less than 525 nm (cyan color line in **figure 1**), the forward scattering spectrum is higher than the backscattering spectrum; values of

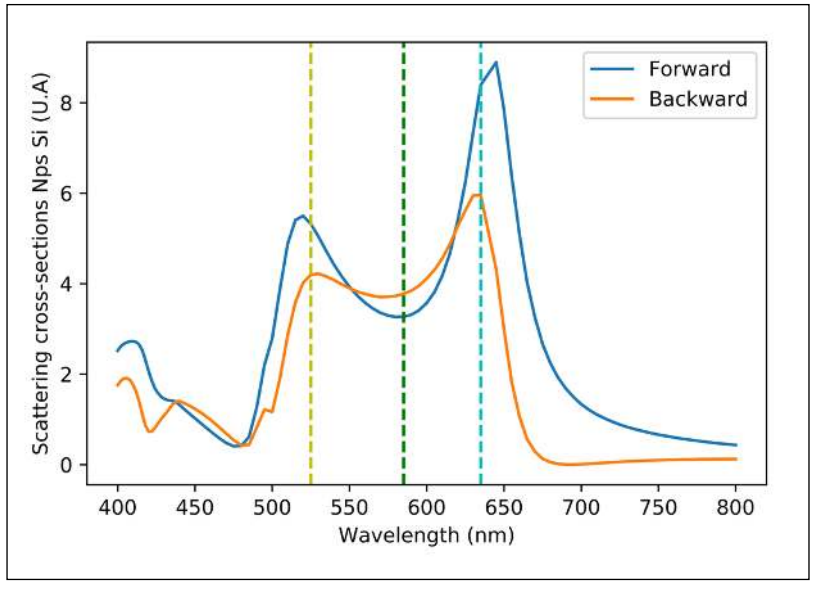

Figure 1. Forward and backward scattering cross-sections for Si nanoparticle with a size of 80 nm

Rev. Acad. Colomb. Cienc. Ex. Fis. Nat. 44(173):974-983, octubre-diciembre de 2020
doi: https://doi.org/10.18257/raccefyn.1265

550 nm and 620 nm for backscattering and forward scattering will occur in approximately equal amounts. At 585 nm (green line in **figure 1**), the magnitude of the backscattering spectrum is higher than in the forward scattering spectrum.

To corroborate these results, the irradiance scattered by a spherical particle with a radius of 80 nm and a refractive index of silicon in free space was analyzed in polar and spherical coordinates varying the wavelength.

As shown in **figures 1, 2,** and figure **1S,** https://www.raccefyn.co/index.php/raccefyn/article/view/1265/2886; the scattering of the spherical particle is approximately the same for wavelengths shorter than 525 nm. However, for wavelength values at which the backward and forward scattering spectra are similar, backscattered irradiance predominates.

As shown in **figure 2S,** https://www.raccefyn.co/index.php/raccefyn/article/view/1265/2887; the scattering by the particle occurs in higher quantity towards the rear, thus generating a backscatter antenna.

As shown in **figure 3S,** https://www.raccefyn.co/index.php/raccefyn/article/view/1265/2888; the nanoparticle scattering generated mainly goes forward, thus forming a directional nanoantenna with a forward scatter pattern and a gain factor close to 11.

In silicon nanoparticle synthesis, methanol, ethanol, and butanol are often used as solvents in the reaction to obtain the nanoparticles (**Cornejo-Monroy, *et al.,*** 2009). To compare the radiation patterns of the silicon nanoparticles suspended in different media, the absorption and scattering cross-sections spectra for spherical particles of 80 nm suspended in methanol were computed taking as refractive index 1.326. The results can be seen in **figure 3**.

In **figure 3,** three peaks can be observed; at 446 nm in the backscatter there was higher intensity than in the forward scattering, but the difference was not significant. At 500 nm and 645 nm wavelengths, forward scattering was higher than the backscattering.

To analyze the radiation patterns obtained with these resonant values of a silicon nanoparticle with a radius of 80 nm suspended in methanol, the graphs of the irradiance in polar and spherical coordinates were calculated.

In **figure 4**, the resulting radiation pattern for a spherical silicon particle of 80 nm suspended in methanol is shown. **Figure 4a**) shows a forward scattering with a maximum gain close to 6 in the 0º direction. Also, it presents some radiation scattering in a perpendicular direction as observable by the lobes at right angles with a small gain close to 2.5; there is a small backscattering at 180º.

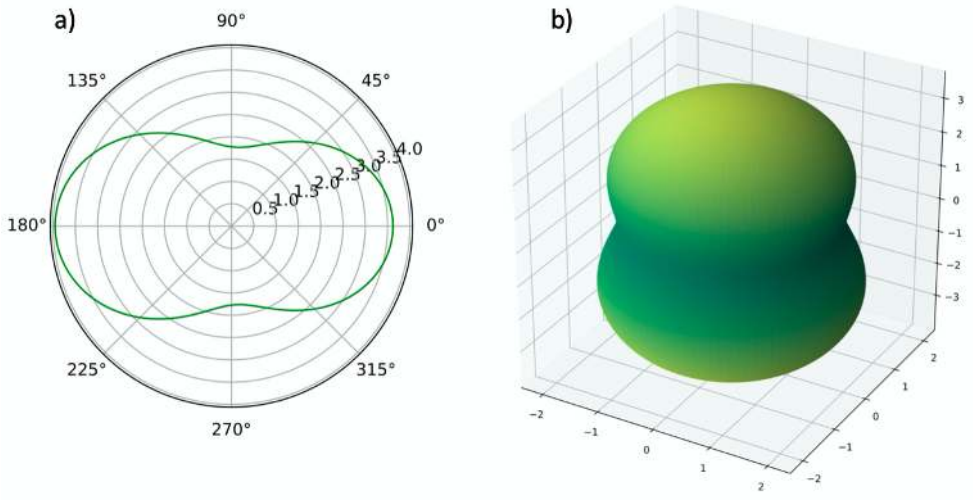

Figure 2. Parallel and perpendicular irradiance of a silicon nanoparticle with a radius of 80 nm, a wavelength of 525 nm, n=4.168, and k=0.036. The radiation pattern represents the scattering of an electric dipole type nanoantenna. **a)** In polar coordinates; **b)** in spherical coordinates

In figures 4S, https://www.raccefyn.co/index.php/raccefyn/article/view/1265/2889 and **5S,** https://www.raccefyn.co/index.php/raccefyn/article/view/1265/2891; the radiation patterns of a silicon nanoparticle with a radius of 80 nm suspended in methanol can be appreciated; the scattering of radiation produced by the nanoparticle is directional forward in a higher amount. In the radiation pattern shown in **figure 4S,** https://www.raccefyn.co/index.php/raccefyn/article/view/1265/2889; the wavelength was 500 nm, the scattering occurred in a higher proportion in a forward direction, but there was also a significant backscatter fraction. Moreover, in **figure 5S,** https://www.raccefyn.co/index.php/raccefyn/article/view/1265/2891; a big forward scatter is observed, but with a broader pattern and less gain compared with the previous case; here, a small fraction backscattered also appears.

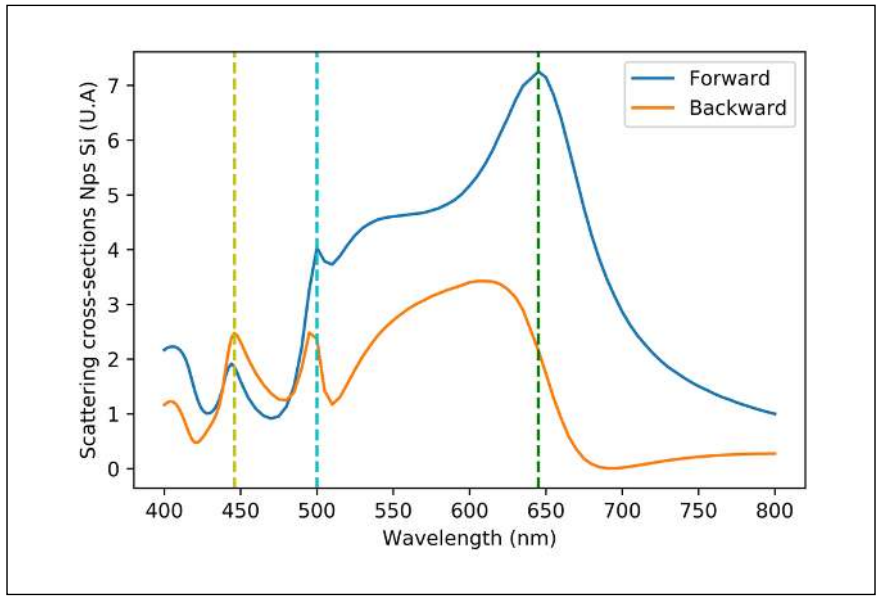

Figure 3. Forward and backward scattering cross-sections of an 80 nm silicon nanoparticle suspended in methanol

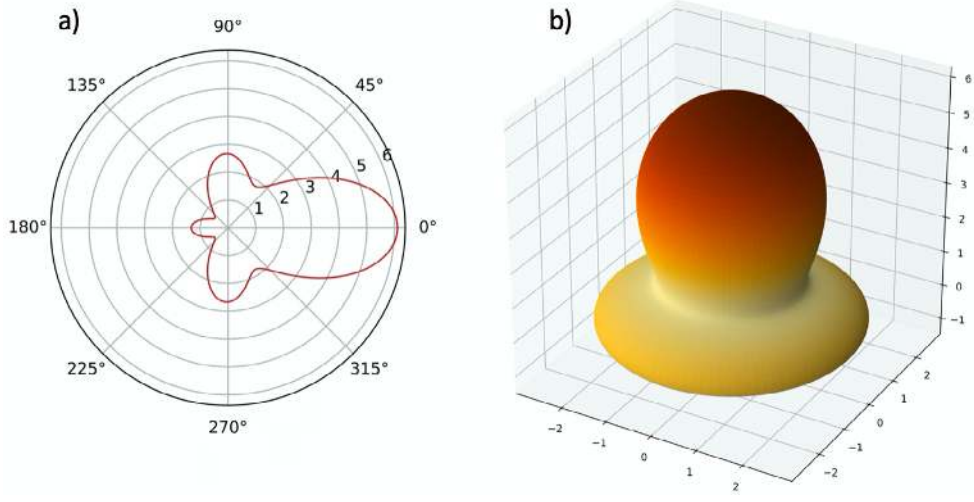

Figure 4. Parallel and perpendicular irradiance of a silicon nanoparticle with a radius of 80 nm suspended in methanol at 446 nm wavelength, n=4.718, and k=0.099. **a)** In polar coordinates and **b)** in spherical coordinates

Rev. Acad. Colomb. Cienc. Ex. Fis. Nat. 44(173):974-983, octubre-diciembre de 2020
doi: https://doi.org/10.18257/raccefyn.1265

For application purposes in the field of nanocircuits, silicon nanoparticles can also become stabilized in quartz. To register the behavior of the scattering of the silicon nanoparticles, the scattering cross-section in quartz was calculated for the refractive index of 1.544, as shown in **figure 5.**

Figure 5 shows the existence of three peaks very similar to those seen in Figure 3, but they differ in that the gap between the scattering peaks forward and backward increased.

To observe the scattering behavior of the silicon nanoparticles in quartz, a scattered irradiance graph was done for each of the wavelength values corresponding to the peak values.

Figure 6 shows the radiation pattern produced by an 80 nm radius silicon nanoparticle in quartz. The graphs also show a narrow directed frontal lobe that concentrates the radiation mostly as a solid angle lower than π/4 radians, as well as a peculiar feature in the radiation pattern, namely the existence of a small fraction of backscattering and the occurrence of a perpendicular scattering directed at π/2 radians.

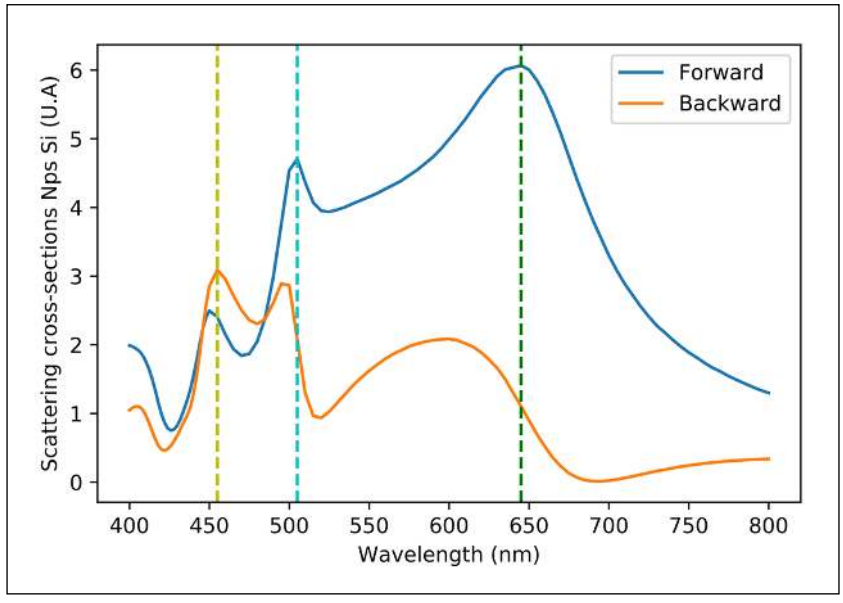

Figure 5. Forward and backward scattering cross-sections for a nanoparticle with a size of 80 nm in quartz

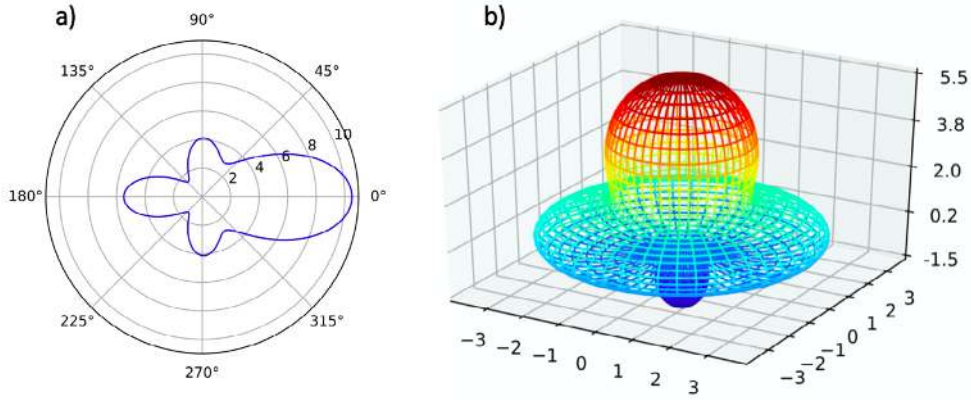

Figure 6. Parallel and perpendicular irradiance of an 80 nm radius silicon nanoparticle in quartz with a wavelength of 455 nm, n=4.622, and k=0.085. **a)** In polar coordinates and **b)** in spherical coordinates

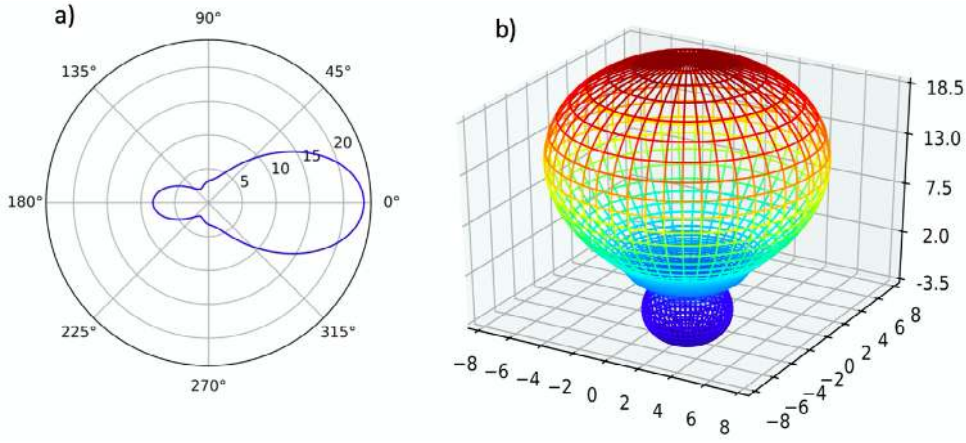

Figure 7. Parallel and perpendicular irradiance of an 80 nm radius silicon nanoparticle in quartz with a wavelength of 505 nm, n=4.262, and k=0.045. **a)** In polar coordinates and **b)** in spherical coordinates

In **figure 7** and figure **6S,** https://www.raccefyn.co/index.php/raccefyn/article/view/1265/2892; showing the irradiance of an 80 nm radius silicon nanoparticle in quartz, the scattering of the radiation is mainly forward. The pattern in **figure 7** shows a higher directivity and gain than the one in **figure 6S,** https://www.raccefyn.co/index.php/raccefyn/article/view/1265/2892; where a more narrowing lobe in the horizontal plane than in the vertical plane can be observed, which means that there is more directivity in this plane. **Figure 6S,** https://www.raccefyn.co/index.php/raccefyn/article/view/1265/2892; shows higher homogeneity of the radiation pattern; in any case, the radiation is directed frontally with a gain of 13. The existence of some of the anomalous scattering present in these nanoparticles is due to the joint appearance of electronic and magnetic orthogonal dipole resonances, which influence the radiation pattern resulting from the spherical nanoparticle.

Conclusions

The Mie scattering study of dielectric nanoparticles was done taking as reference 80 nm silicon nanoparticles suspended in different media to analyze their radiation patterns and the characteristics obtained in various suspension media, as well as their possible applications in nanoantennas. Based on the results it can be concluded that the radiation patterns, their directivity, and the gain of the incident radiation on a dielectric particle can be anticipated and addressed numerically knowing relevant data such as the dielectric constants of the materials, the shape, and the size of the nanoparticles, allowing a useful tool in the practical design of nanoantennas for future applications in nanotechnology systems. **Figure 2,** figure 1S, https://www.raccefyn.co/index.php/raccefyn/article/view/1265/2886; figure 2S, https://www.raccefyn.co/index.php/raccefyn/article/view/1265/2887; figure 3S, https://www.raccefyn.co/index.php/raccefyn/article/view/1265/2888; **figure 4,** figure 4S, https://www.raccefyn.co/index.php/raccefyn/article/view/1265/2889; figure 5S, https://www.raccefyn.co/index.php/raccefyn/article/view/1265/2891; **figure 6, figure 7,** and figure 6S, https://www.raccefyn.co/index.php/raccefyn/article/view/1265/2892 show the exclusive results of the study, especially for the case of 80 nm silicon nanoparticles suspended in three different media.

Knowing the dimensions of the nanoparticles and the dielectric constants of the materials used, and developing the necessary numerical calculations and using the scattering spectra it was possible to visualize the radiation patterns of the silicon nanoparticles in polar and spherical coordinate systems at different wavelengths, which allowed for the analysis of the shape and the predominant scattering in a spherical silicon nanoparticle suspended in different material media (vacuum, methanol, quartz).

Rev. Acad. Colomb. Cienc. Ex. Fis. Nat. 44(173):974-983, octubre-diciembre de 2020
doi: https://doi.org/10.18257/raccefyn.1265

The anisotropic scattering in silicon nanoparticles suspended in different media, which can be caused by the interference of electric and magnetic dipoles induced by the incident electromagnetic radiation, was demonstrated using the calculus of Mie theory formulas.

The radiation patterns of the nanoparticles strongly depend on the shape and the size of the nanoparticle, the dielectric constants of the materials, and the surrounding media. When analyzing **figures 1, 3, and 5** showing the scattering cross-sections for silicon nanoparticles, it can be observed that if the incident electromagnetic radiation is in the visible spectral range, increasing the refractive index of the medium containing the nanoparticles of silicon will send forward most of the scattered energy.

These results may be useful when including nanoparticles in nanotechnology applications such as nanoantennas, lens-type systems, the concentration of radiation on quantum dots, the focusing of light in photonic devices and solar cells, and in the study of samples in nano-spectroscopy.

Supplementary information

Figure 1S. Parallel and perpendicular irradiance of a silicon nanoparticle with a radius of 80 nm, with a wavelength of 550 nm, n = 4.075, and k = 0.029. For wavelengths of 620 nm, n = 3.893 and k = 0.017 the irradiance graph is similar, **a)** in polar coordinates **b)** in spherical coordinates. See the figure 1S in https://www.raccefyn.co/index.php/raccefyn/article/view/1265/2886

Figure 2S. Parallel and perpendicular irradiance of a Silicon nanoparticle with radius 80nm, with a wavelength of 585nm, n=3.971 y k=0.022, **a)** in polar coordinates **b)** in spherical coordinates. See the figure 2S in https://www.raccefyn.co/index.php/raccefyn/article/view/1265/2887

Figure 3S. Parallel and perpendicular irradiance of a Silicon nanoparticle with radius 80 nm, with a wavelength of 660 nm, n=3.828, and k=0.014. **a)** in polar coordinates **b)** in spherical coordinates. See the figure 3S in https://www.raccefyn.co/index.php/raccefyn/article/view/1265/2888

Figure 4S. Parallel and perpendicular irradiance of a suspended in methanol silicon nanoparticle with a radius of 80 nm, at 500 nm wavelength, n=4.290, and k=0.047. **a)** in polar coordinates **b)** in spherical coordinates. See the figure 4S in https://www.raccefyn.co/index.php/raccefyn/article/view/1265/2889

Figure 5S. Parallel and perpendicular irradiance of a suspended in methanol silicon nanoparticle with a radius of 80 nm, at 645 nm wavelength, n=3.850, and k=0.015. **a)** in polar coordinates **b)** in spherical coordinates. See the figure 5S in https://www.raccefyn.co/index.php/raccefyn/article/view/1265/2891

Figure 6S. Parallel and perpendicular irradiance of a Silicon nanoparticle with a radius of 80 nm in quartz, with a wavelength of 645 nm, n=3.850, and k=0.015. **a)** in polar coordinates **b)** in spherical coordinates. See the figure 6S in https://www.raccefyn.co/index.php/raccefyn/article/view/1265/2892

Author contribution

Both authors contributed to the research and writing of the code to carry out the numerical calculations, to the analysis of the data obtained, and to the final drafting of the manuscript.

Conflicts of interest

There are no conflicts of interest to declare.

References

Biagioni, P., Huang, J. S., Hecht, B. (2012). Nanoantennas for visible and infrared radiation, Reports on Progress in Physics. **75** (2): 024402.

Bohren, C. F., Huffman, D. R. (2008). Absorption and scattering of light by small particles, New York, USA: John Wiley & Sons.

Cornejo-Monroy, D., Sánchez-Ramírez, J. F., Pescador Rojas, J. A., Herrera-Pérez J. L., González-Araoz, M. P., Guarneros, C. (2009). Nanoesferas monodispersas de SiO2: síntesis controlada y caracterización, Superficies y vacío. **22** (3): 44-48.

Decker, M., Staude, I. (2016). Resonant dielectric nanostructures: a low-loss platform for functional nanophotonics, Journal of Optics. **18** (10):103001.

Evlyukhin, A. B., Novikov, S. M., Zywietz, U., Eriksen, R. L., Reinhardt, C., Bozhevolnyi, S. I., Chichkov, B. N. (2012). Demonstration of magnetic dipole resonances of dielectric nanospheres in the visible region. Nano letters. **12** (7): 3749-3755.

Fu, Y. H., Kuznetsov, A. I., Miroshnichenko, A. E., Yu, Y. F., Luk'yanchuk, B. (2013). Directional visible light scattering by silicon nanoparticles. Nat, Commun. **4:** 1527.

Kerker, M., Wang, D. S., Giles, C. L. (1983). Electromagnetic scattering by magnetic spheres, JOSA. **73** (6): 765-767.

Kuznetsov, A. I., Miroshnichenko, A. E., Fu, Y. H., Zhang, J., Luk'Yanchuk, B. (2012). Magnetic light, Scientific reports. **2:** 492.

Kuznetsov, A. I., Miroshnichenko, A. E., Brongersma, M. L., Kivshar, Y. S., Luk'yanchuk, B. (2016). Optically resonant dielectric nanostructures, Science. **354** (6314): aag2472.

Luk'yanchuk, B., Zheludev, N. I., Maier, S. A., Halas, N. J., Nordlander, P., Giessen, H., Chong, C. T. (2010). The Fano resonance in plasmonic nanostructures and metamaterials, Nature materials. **9** (9): 707-715.

Mongia, R. K., Bhartia, P. (1994). Dielectric resonator antennas—A review and general design relations for resonant frequency and bandwidth, International Journal of Microwave and Millimeter-Wave Computer-Aided Engineering. **4** (3): 230-247.

Novotny, L., Van Hulst, N. (2011). Antennas for light, Nature photonics. **5** (2): 83-90.

Tribelsky, M. I., Geffrin, J. M., Litman, A., Eyraud, C., Moreno, F. (2015). Small dielectric spheres with high refractive index as new multifunctional elements for optical devices, Scientific reports. **5:** 12288.